Phase Equilibrium and Crystallization Behavior of Mixed Lipid Systems

Baomin Liang, Yuping Shi, and Richard W. Hartel*

Department of Food Science, University of Wisconsin–Madison, Madison, Wisconsin 53706

ABSTRACT: As complex lipid systems, the phase and crystallization behavior of mixtures of a high-melting milk fat fraction with a low-melting milk fat fraction or canola oil was studied. A turbidity technique was developed to estimate solubility and metastability conditions of these lipid mixtures. Both solubility and metastability of the high-melting milk fat fraction in liquid lipids increased exponentially with temperature. At a given equilibration temperature, liquid phases and solid fractions with nearly identical melting profiles and TAG compositions were obtained regardless of the original concentration of the lipid mixture. The maximum melting temperature (MMT), as measured by DSC, of the liquid phase increased dramatically in the equilibrium temperature range of 27.5–35.0°C but did not change at temperatures below and above this range (down to 25.0°C and up to 40°C in this study). The content of long-chain TAG (C_{46}–C_{52}) increased and short-chain TAG (C_{36}–C_{40}) decreased in the liquid phases as the equilibrium temperature increased. A plot of the TAG group ratio (i.e., long-/short-chain TAG) vs. equilibrium temperature was generated to illustrate the phase behavior of the complex lipid system and to represent a solubility curve, from which the supersaturation level for crystallization kinetics was determined. Higher supersaturation and lower temperature resulted in higher nucleation and crystallization rates. Compared to the system with a low-melting milk fat fraction, mixtures of the high-melting milk fat fraction with canola oil had higher nucleation and crystallization rates due to the lower solubility found for this system.

Paper no. J9927 in *JAOCS 80,* 301–306 (April 2003).

KEY WORDS: Canola oil, crystallization, kinetics, lipid, metastability, milk fat, phase behavior, phase equilibrium, solubility, turbidity.

Natural lipids generally contain a wide range of component TAG, depending on source and origin. FA, as constituent parts of a TAG, show variation to different extents for different natural lipids. For example, cocoa butter, a relatively simple fat, has about four major FA (1), whereas milk fat, a complex lipid, contains more than 400 FA that constitute over 200 TAG species, with none present at levels greater than 4–5 mol% (2,3). When two lipids are mixed, as often occurs in food products, it is extremely difficult to predict phase behavior and crystallization kinetics. For milk fat, it is generally accepted that there are three major TAG groups (low-, medium-, and high-melting) that behave (e.g., melt, crystallize) somewhat independently (4). Some of the glycerides with high m.p. may dissolve in other glycerides of lower m.p. (5). In addition, the phenomenon of intersolubility, where two or more TAG species can cocrystallize and form compound crystals (or mixed crystals), exists in complex lipid systems (6,7). Therefore, such complex lipid mixtures may have characteristics of both melt and solvent systems.

Because of the complexity of TAG composition and crystallization of natural lipid systems, such as mixtures containing milk fat, many factors can influence the kinetics of crystallization. Supersaturation or undercooling, as the driving force for crystallization, plays the most important role. However, it is very difficult to determine solubility (or the saturation level) or a single, thermodynamically meaningful m.p. for complex lipid systems. For example, milk fat exhibits a melting range from −40 to 40°C owing to the wide range of TAG (or FA) species. Thus, it is not feasible to use the concentration and/or m.p. of a single TAG to evaluate supersaturation and undercooling in complex lipids.

The concept of metastability is also very important to crystallization kinetics since it is directly related to the induction time for onset of nucleation. The existence of a metastable state, where the lipid is undercooled but does not crystallize over some finite time scale, is common for most lipid systems, including milk fat. The metastable zone width affects the choice of processing conditions since the lipid system must be cooled to the point where sufficient supersaturation is created for the given process. However, the metastable zone width is dependent on processing conditions, such as temperature, agitation rate, and presence of impurities (9).

In this work, the solubility and metastable zone of a high-melting milk fat fraction in either low-melting milk fat fraction or canola oil were studied by using a turbidimetric technique. The crystallization behavior of these lipid systems, also measured by turbidimetry, was then correlated to the supersaturation driving force.

EXPERIMENTAL PROCEDURES

High- and low-melting milk fat fractions (labeled as 28S and 16L, respectively) were obtained from the first and third stages of a three-stage fractionation of anhydrous milk fat with crystallization temperatures of 28 and 15.5°C, respectively, performed at the Center for Dairy Research, University of Wisconsin–Madison, on a pilot-scale batch crystallization system. The canola oil (labeled CNL) was a salad oil product obtained from C&T Quincy (Charlotte, NC). The temperatures of the peak of the highest-melting endotherm (maximum melting temperature; MMT) obtained by DSC (DSC 7; PerkinElmer, Norwich, CT) for 10 mg of sample at a heating rate of 5°C/min were 45.4, 14.6, and −18°C for 28S, 16L, and CNL, respectively. The TAG composition, in terms of acyl carbon number, of the materials was determined based

*To whom correspondence should be addressed.
E-mail: hartel@calshp.cals.wisc.edu

on the method of Lund (10), with minor modification. A Hewlett-Packard 5890 GC system (Wilmington, DE) was used, and the results are shown in Table 1.

Under certain circumstances, the high-melting components of a complex lipid system may be treated as a solute and the low-melting components treated as solvent. If this is the case, the solubility of the high-melting milk fat fraction in a liquid oil at a certain temperature is the maximum amount of the hard lipid that can be dissolved in the liquid oil. Beyond this solubility concentration, solid and liquid phases coexist. Metastability of the high-melting milk fat fraction in a liquid oil at a certain temperature was defined as the maximum content of the hard lipid in the system, at which the supersaturated liquid state was maintained without any phase transition for an extended period of time (7 d for systems studied in this work).

To obtain phase equilibrium, solidified 28S was added to the liquid oil (16L or CNL) at different ratios at room temperature. The appropriate lipids (100 g) were mixed in a 250-mL Erlenmeyer flask, which was placed in a bath at the desired equilibration temperature, and agitated (100 rpm) for at least 5 d. If the concentration of the solid phase was higher than the solubility level, solid–liquid phase equilibrium would be established with the excess solid phase found as a dispersion. If the 28S concentration was below the solubility level, the solid lipid would be completely dissolved. An effective solubility was determined as the concentration of the high-melting milk fat fraction where all of the solid phase had dissolved, as determined by a sharp break in turbidity. That is, at concentrations slightly higher than this solubility, turbidity was high, whereas at concentrations just below this solubility, the turbidity was essentially zero since no crystals remained in solution. Initially, eight large steps in concentration (2 to 3%) were used to determine the general range of phase equilibrium. Subsequent measurements were done in the pertinent range, over which turbidity changed from zero, by using eight smaller concentration increments (0.4 to 1.0%) to determine the turning point of turbidity more accurately.

TABLE 1
TAG Composition (g/100 g identified TAG) of High-Melting Milk Fat Fraction (28S), Low-Melting Milk Fat Fraction (16L), and Canola Oil (CNL)

Acyl carbon number	28S	16L	CNL
≤26	0.70	1.54	0.43
28	0.45	0.81	0.00
30	0.84	1.59	0.00
32	1.77	3.04	0.00
34	4.15	6.72	0.00
36	7.30	12.01	0.32
38	11.24	19.35	5.00
40	7.08	11.32	0.00
42	5.86	6.57	0.00
44	6.76	4.83	0.00
46	9.11	3.17	0.28
48	12.40	5.58	0.00
50	16.41	8.64	2.86
52	10.94	8.60	11.32
54	4.98	6.22	79.80

To determine the limits of the metastable state, mixtures of the liquid oils (100 g) with different concentrations of 28S higher than the solubility were melted in an Erlenmeyer flask at 70–90°C for 30 min to destroy crystal memory, cooled to the test temperature, and agitated (100 rpm) with a magnetic stir bar in the water bath for at least 7 d. If the concentration was higher than the metastability concentration, the existing metastable state would be broken, and solid and liquid phases would coexist. Otherwise, the system would remain in the supersaturated, metastable state. Again, the turbidity change between these two states was used to determine the point of metastability, and a two-step approach with different increments of concentration was used to accurately determine the turning point of turbidity.

Technically, measuring a true solubility concentration requires both equilibration by dissolution of solids and equilibration by crystallization to a final end point. Comparison of solubility concentration by these two approaches (from above and below) ensures that true phase equilibrium has been attained and that no kinetic constraints inhibit the measurements. In this study, the equilibrium condition was approached from only one direction (by dissolution), so final concentrations of 28S in 16L may not represent the true thermodynamic equilibrium as a result of kinetic limitations. Also, the 28S fraction is not a completely crystalline solid but contains some liquid oil entrained within the crystals. No attempt was made to separate these components in this work.

After establishing the phase equilibrium or metastable state, turbidity was measured on a Beckman DU-65 spectrophotometer (Beckman-Coulter, Inc., Fullerton, CA). Turbidity of the lipid mixture increased sharply when crystals were present in the liquid phase, as shown in Figure 1. Solubility and metastability were determined as the concentration corresponding to the turning point on the plot of turbidity vs. concentration at a given temperature. The liquid–solid system was then separated by use of vacuum filtration with Whatman #4 paper, and both phases were analyzed for TAG composition *via* GC and for melting profile by DSC from –50 to 80°C at a heating rate of 5°C/min.

Crystallization kinetics were determined by using a turbidity technique based on the fact that after the onset of crystallization, as the number and size of crystals increased, the turbidity of the system increased. A mixture of 28S and 16L (or CNL) was melted at about 80°C for 30 min and then cooled to the crystallization temperature (25.0 and 27.5°C in this work) in a walk-in constant temperature chamber for measurement of spontaneous nucleation and static crystal growth rates. The change in turbidity of the system during crystallization was measured on a Bausch & Lomb (Rochester, NY) Spectronic 20 spectrophotometer. The crystallization rate expressed as the rate of change of turbidity over time was determined by regression of the linear part of the turbidity–time curve for the crystallization.

RESULTS AND DISCUSSION

Both solubility and metastability of 28S in 16L or canola oil increased as the temperature increased (Fig. 2). Regression

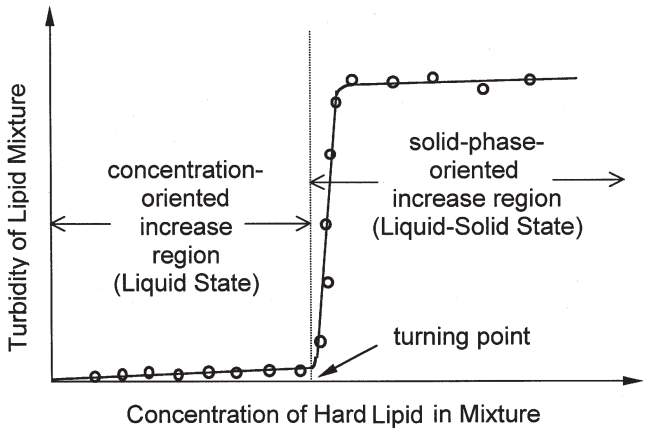

FIG. 1. Principle for determination of solubility and metastability of the high-melting milk fat fraction in liquid oils. Symbols represent data points at different ratios of high-melting milk fat fraction.

analysis was performed to fit the data to an exponential model, expressed as Equation 1:

$$C_{S/M} = k \exp(aT) \quad [1]$$

where $C_{S/M}$ is the solubility (S) or metastability (M) of 28S in liquid oil, (28S wt%) or (grams C_{46}–C_{52})/(grams $\leq C_{40}$); k is a dimensionless coefficient; a is a coefficient with dimensions of 1/°C; and T is temperature (°C).

The regression results are shown in Table 2 and compared to the experimental data in Figure 2. The solubility and metastability concentrations of 28S in low-melting milk fat fraction (16L) are higher than those in canola oil at any temperature, owing to the similarity of TAG molecules in 28S and 16L. In this case, the greater similarity in molecules between milk fat components led to higher levels of solubility than for the 28S–canola system, although the temperature dependence was similar between the two fat systems. The metastable zone for these fat mixtures decreased as temperature decreased. However, the determination of metastability depends to a large extent on the method of measurement. Allowing longer time periods (greater than 7 d) of mixing in the supersaturated state would lead to lower metastable zone widths.

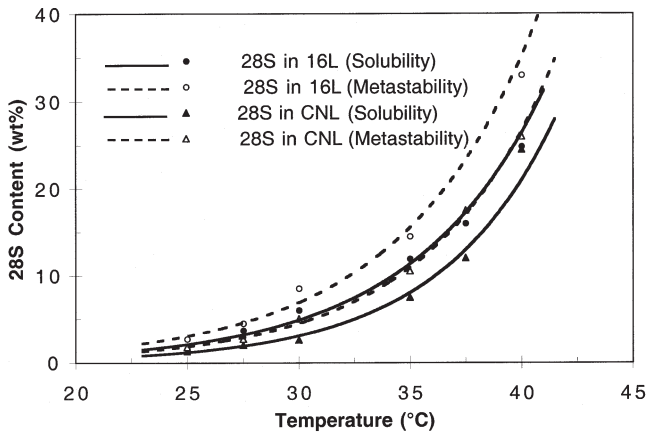

FIG. 2. Effective solubility (solid lines) and metastability (dashed lines) of a high-melting milk fat fraction (28S) in a low-melting milk fat fraction (16L) and canola oil (CNL) at different temperatures.

TABLE 2
Regression Results for Exponential Model (Eq. 1)[a]

Fats	S/M[b]	k	a	R^2
28S	*S*	0.0305	0.161	0.971
28S in CNL	*S*	0.0096	0.192	0.989
28S in 16L	*M*	0.0511	0.163	0.985
28S in CNL	*M*	0.0212	0.178	0.997

[a]Regression was performed at a confidence level of 95%.
[b]*S,* solubility; *M,* metastability. For other abbreviations see Table 1.

If some of the high-melting fraction is dissolving in the low-melting component, the liquid should have a different melting profile and composition after equilibration at different temperatures. Figure 3 shows the melting profiles of equilibrated liquid phases in the 28S–16L system at different temperatures. Different TAG groups were contained in the liquid phase, depending on the temperature of equilibration. At temperatures of 30°C or below, a single peak with m.p. of about 15°C was observed. This corresponded to the pure 16L liquid fat, the solvent, since very little of the 28S was soluble at this temperature (Fig. 2) and the high-melting components had all crystallized out of solution. At temperatures above 30°C, a new TAG group with higher m.p. appeared owing to the presence of the 28S fraction that remained dissolved in the solvent. The MMT values (maximum peak temperature in the DSC scan) of the liquid phase increased dramatically, from about 15 to 35°C over the equilib-

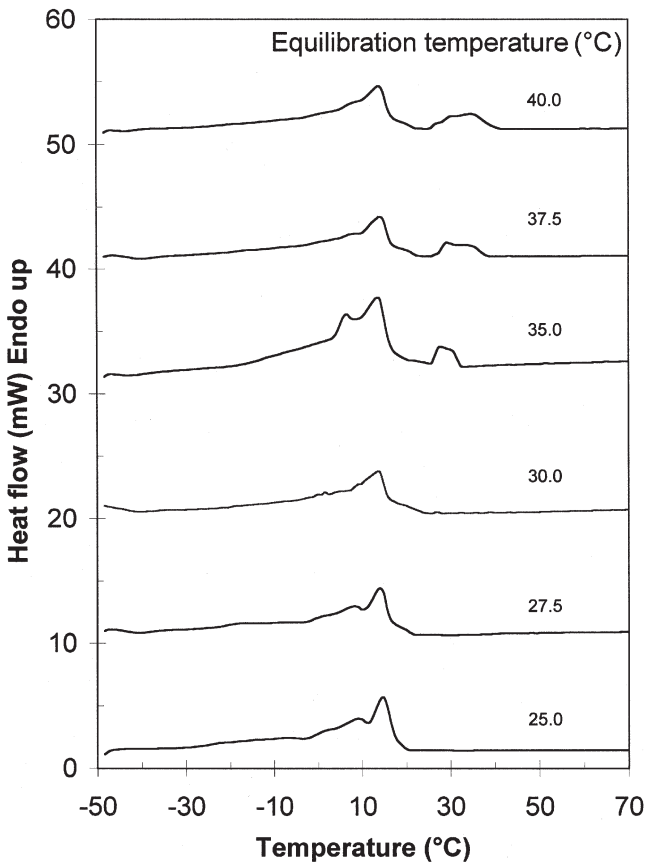

FIG. 3. Melting profiles from DSC of liquid phases of a high-melting milk fat fraction (28S) in a low-melting milk fat fraction (16L) at different equilibration temperatures. The liquid phase was separated from the slurry by vacuum filtration and cooled to –50°C before scanning at 10°C/min to obtain a melting curve.

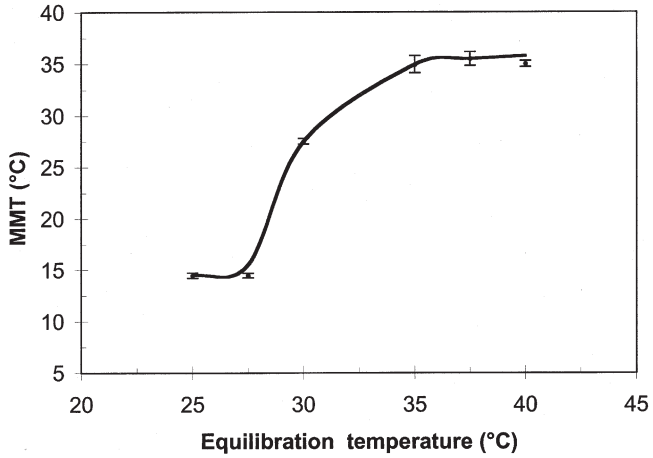

FIG. 4. Maximum melting temperature (MMT) from DSC of liquid phases obtained after equilibration of a high-melting milk fat fraction (28S) with a low-melting milk fat fraction (16L) at different temperatures. Error bars represent SD.

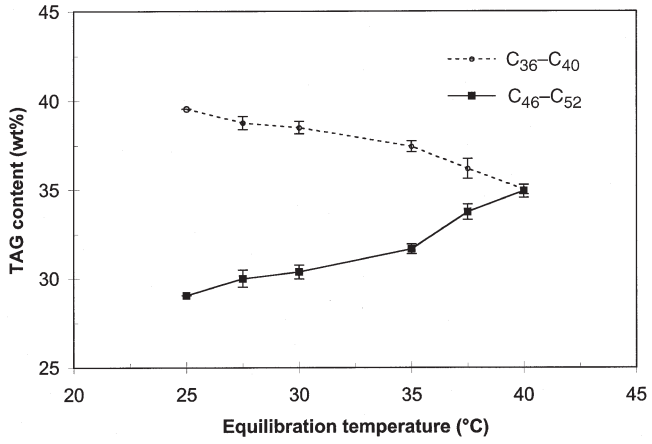

FIG. 5. Concentration of TAG groups C_{36}–C_{40} and C_{46}–C_{52} in liquid phases for a high-melting milk fat fraction (28S) equilibrated with a low-melting milk fat fraction (16L) at different temperatures. Error bars represent SD.

rium temperature range of 27.5 to 35.0°C, but did not change at temperatures below and above this range (Fig. 4). Thus, the liquid phase experienced a change from containing one major TAG group (at lower temperatures where all of the high-melting component had crystallized out) to containing two TAG groups as temperature increased through this range.

The changes in TAG composition for 28S equilibrated in 16L at different temperatures are shown in Figure 5. The liquid phase had an increased content of long-chain TAG group (C_{46}–C_{52}) and decreased short-chain TAG (C_{36}–C_{40}) as the equilibration temperature increased. The chemical composition changed gradually with the equilibration temperature. This means that for this milk fat system, there were specific TAG compositions in the liquid and solid phases after phase equilibrium had been attained at a certain temperature. Table 3 shows that the ratios of certain TAG changed according to crystallization temperature. At higher temperatures of equilibration, more of the higher acyl carbon number TAG remained in the liquid phase.

Note that at each crystallization temperature, the composition of solid and liquid phases was independent of the initial starting composition (28S in 16L), as seen in Table 3. Multiple samples with different ratio of 28S to 16L gave similar results for both liquid and solid phase composition, as shown by the small SD in Table 3. Also, the ratios of specific TAG groups were quite consistent regardless of the initial ratio of 28S to 16L.

At each temperature, there were certain ratios among TAG components in the equilibrated liquid phases and solid fractions (Table 3). The ratios C_{38}/C_{36} and C_{40}/C_{36} were essentially constant at 1.30 and 1.03, respectively, in both liquid phases and solid fractions for the equilibration temperature range from 25 to 40°C. This result implies that the short-chain TAG group (C_{36}–C_{40}) might behave like a single entity, which was the major component of the solvent portion in the liquid phase and was entrained as an entity (a solvent) into the solid phases. In addition, the ratios between C_{52}, C_{50}, and C_{46} to C_{48} in the liquid phases or solid fractions had different specific values over the equilibration temperature ranges of 25 to 30°C and 35 to 40°C, respectively. For example, the solid fractions obtained in the equilibration temperature range from 25 to 30°C had specific ratios for C_{52}, C_{50}, and C_{46} to C_{48} of 0.93, 1.14, and 0.82, and the corresponding liquid phases (after equilibration) had the same melting point of 14.5°C. The solid fractions obtained in the equilibration temperature range from 35 to 40°C had different specific ratios of C_{52}, C_{50}, and C_{46} to C_{48} of ~1.50, 1.50, and 0.67, and the corresponding equilibrated liquid phases had a m.p. of about 35°C (see also Fig. 4). It seems that two types of solid phase having different and relatively stable TAG group (C_{46}–C_{52}) compositions were related to the peak areas on the DSC melting curve of corresponding liquid phases. Essentially, the TAG groups (C_{36}–C_{40}) and (C_{46}–C_{52}) behaved like two entities to construct different liquid phases having different proportions of (C_{46}–C_{52})/(C_{36}–C_{40}). These characteristics implied that in milk fat systems, long-chain, saturated TAG behaved like solutes, whereas short-chain and unsaturated TAG behaved like solvents. Although the crystallization behavior of milk fat is very complex, since the TAG can exist in multiple crystalline states, the materials in milk fat may, to a first approximation, be considered as distinct lipid phases. These lipid phases may be considered as solvent and solute in a binary system over a limited temperature range of particular importance to milk fat fractionation.

To apply the concept that certain long-chain, saturated TAG behave like solutes and short-chain and unsaturated TAG behave like solvents, the relative mass ratio of the key long-chain TAG (C_{46}–C_{52}) to short-chain TAG ($\leq C_{40}$) [g (C_{46}–C_{52})/g ($\leq C_{40}$)] was used to express the concentration of crystallizing species in this milk fat system. In this way, the phase equilibrium of this complex lipid system can be simplified, and the solubility of high-melting TAG (solute) in low-melting TAG (solvent) can be interpreted, as shown in Figure 6. Any milk fat system, whether summer or winter milk fat, can be located on the solubility plot according to its TAG composition. Hence, the supersaturation level at a certain temperature can be determined from the difference between the TAG ratio and the solubility value at that temperature. In Figure 6, the winter milk fat has a higher TAG ratio at 27.5°C than summer milk fat and thus would be more supersaturated.

TABLE 3
Chemical Composition of Liquid Phase and Solid Fraction in Terms of Milk Fat Groups and Ratios at Different Equilibration Temperatures

ET[a] (°C)	25.0	27.5	30.0	35.0	37.5	40.0
Number of samples[b]	5	6	7	7	8	4
MMT of LP[c] (°C)	14.5 ± 0.3	14.4 ± 0.2	27.5 ± 0.3	35.0 ± 0.8	35.5 ± 0.7	35.0 ± 0.3
MMT of SF[c] (°C)	46.7 ± 0.9	45.9 ± 0.3	49.2 ± 1.2	51.6 ± 1.1	52.6 ± 1.1	53.7 ± 0.4
	Liquid phase (g TAG/100 g identified TAG in sample)					
$\leq C_{40}$	52.2 ± 0.4	51.6 ± 0.4	51.2 ± 0.4	49.9 ± 0.3	47.7 ± 0.6	46.3 ± 0.3
C_{42}–C_{44}	12.2 ± 0.2	12.2 ± 0.1	12.2 ± 0.7	12.3 ± 0.2	12.5 ± 0.3	12.5 ± 0.2
C_{46}–C_{52}	29.3 ± 0.4	30.0 ± 0.5	30.4 ± 0.4	31.7 ± 0.3	33.8 ± 0.4	23.9 ± 0.4
C_{54}	6.3 ± 0.2	6.2 ± 0.2	6.3 ± 0.1	6.2 ± 0.1	6.1 ± 0.4	6.4 ± 0.1
	Liquid phase (TAG ratio)					
C_{38}/C_{36}	1.3 ± 0.0	1.3 ± 0.0	1.3 ± 0.0	1.3 ± 0.0	1.3 ± 0.0	1.3 ± 0.0
C_{40}/C_{36}	1.0 ± 0.0	1.0 ± 0.0	1.0 ± 0.0	1.0 ± 0.0	1.0 ± 0.0	1.0 ± 0.0
C_{46}/C_{48}	1.0 ± 0.0	1.0 ± 0.1	1.0 ± 0.0	1.0 ± 0.0	0.9 ± 0.0	0.9 ± 0.0
C_{50}/C_{48}	1.2 ± 0.0	1.2 ± 0.0	1.2 ± 0.0	1.1 ± 0.0	1.2 ± 0.0	1.2 ± 0.0
C_{52}/C_{48}	1.3 - 1.2	1.3 ± 0.0	1.2 ± 0.0	1.2 ± 0.0	1.1 ± 0.0	1.1 ± 0.0
	Solid fraction (g TAG/100 g identified TAG in sample)					
$\leq C_{40}$	33.0 ± 1.0	35.1 ± 0.2	29.2 ± 1.7	33.0 ± 1.1	29.6 ± 1.4	30.4 ± 0.7
C_{42}–C_{44}	11.4 ± 0.3	11.4 ± 0.1	10.5 ± 0.4	9.4 ± 0.4	9.4 ± 0.3	9.4 ± 0.8
C_{46}–C_{52}	49.6 ± 0.7	47.3 ± 0.2	54.4 ± 2.1	51.0 ± 1.3	63.1 ± 0.8	51.5 ± 0.4
C_{54}	6.0 ± 0.6	6.3 ± 0.1	5.9 ± 0.9	7.6 ± 0.5	8.0 ± 0.7	8.8 ± 0.3
	Solid fraction (TAG ratio)					
C_{38}/C_{36}	1.3 ± 0.0	1.3 ± 0.0	1.3 ± 0.0	1.3 ± 0.0	1.0 ± 0.0	1.3 ± 0.0
C_{40}/C_{36}	1.0 ± 0.0	1.0 ± 0.0`1.0 ± 0.01.0 ± 0.0		0.7 ± 0.0	1.0 ± 0.0	
C_{46}/C_{48}	0.8 ± 0.0	0.8 ± 0.0	0.8 ± 0.0	0.7 ± 0.0	0.6 ± 0.0	0.7 ± 0.0
C_{50}/C_{48}	1.1 ± 0.1	1.2 ± 0.0	1.2 ± 0.0	1.4 ± 0.1[d]	1.5 ± 0.1	1.5 ± 0.0
C_{52}/C_{48}	0.9 ± 0.1	1.0 ± 0.0	0.9 ± 0.0	1.2 ± 0.1[d]	1.5 ± 0.2	1.5 ± 0.1

[a]ET, equilibration temperature.
[b]Number at each temperature representing equilibrated systems having different ratios of high-melting (28S) to low-melting (16L) materials.
[c]MMT, maximum melting temperature; LP, liquid phase; SF, solid fraction.
[d]Unsatisfactory data due to additional crystallization during filtration at lower temperature.

The crystallization kinetics for mixtures containing 28S and either 16L or canola oil were related to the driving force (i.e., supersaturation, $C - C_s$) based on the solubility data (Fig. 6). Typical crystallization results are shown in Figure 7. Addition of greater quantities of 28S to CNL resulted in faster crystallization kinetics, as indicated by the more rapid onset and rate of turbidity increase.

A nucleation rate in terms of the inverse of induction time (1/min) and a relative crystallization rate expressed as turbidity change per unit time (1/m-min) were obtained from the starting point of derivative change and the slope of the increasing part of the turbidity plot vs. duration, respectively. The nucleation rate (1/min) and relative crystallization rate (1/m-min) of the mixtures at crystallization temperatures of 25.0 and 27.5°C are shown in Figures 8 and 9. Higher supersaturation and lower temperature resulted in both higher nucleation rate and higher crystallization rate. Compared to the system with 16L, mixtures of 28S with canola oil had higher nucleation and crystallization rates. This is consistent with the lower solubility found for this system.

For the milk fat system (28S in 16L), the crystallization rate was very low when the supersaturation was below a certain level. However, once the supersaturation was higher than this critical value, the crystallization rate increased dramatically. Thus, the power law model was not adequate to express the relation between crystallization rate and supersaturation.

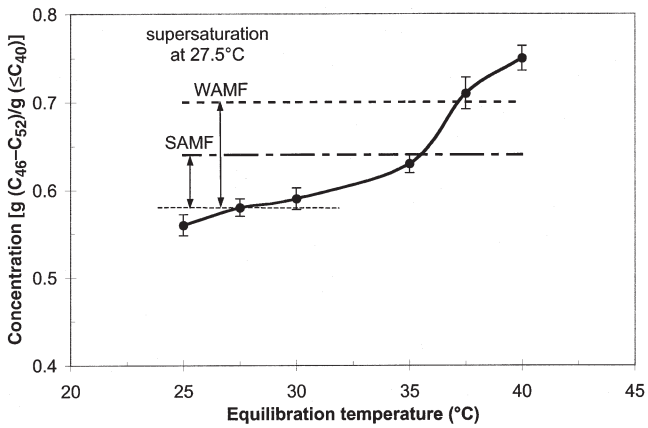

FIG. 6. Effective solubility curve of a high-melting milk fat fraction (28S) in a low-melting milk fat fraction (16L) in terms of the ratio of long-chain (C_{46}–C_{52}) to short-chain ($\leq C_{40}$) TAG. WAMF, winter anhydrous milk fat; SAMF, summer anhydrous milk fat. Error bars represent SD.

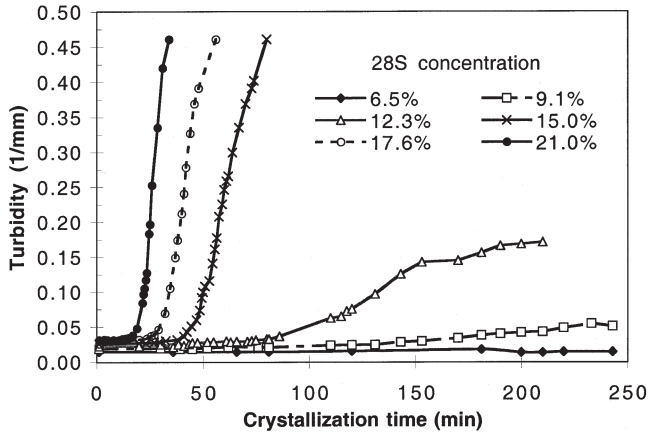

FIG. 7. Change in turbidity with time during crystallization of the high-melting milk fat fraction (28S) at different addition levels in canola oil (CNL) at 25.0°C.

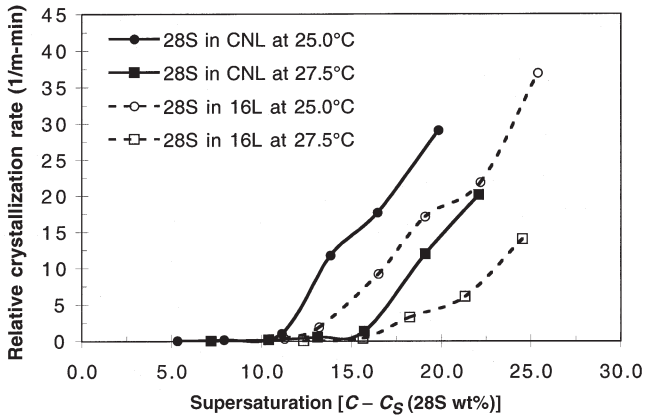

FIG. 9. Crystallization rate vs. supersaturation (in wt%) for lipid mixtures at 25.0 and 27.5°C. For abbreviations see Figure 2.

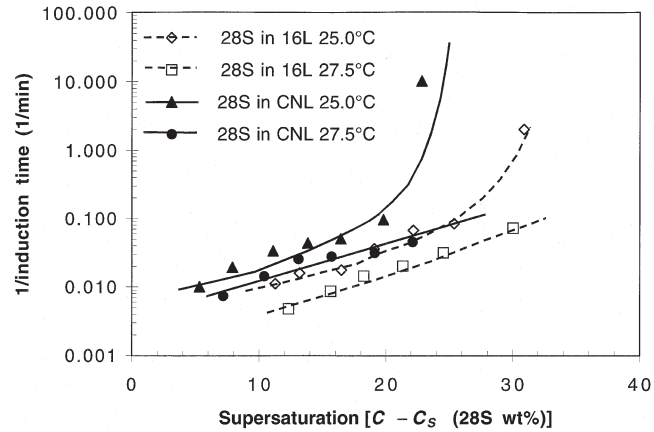

FIG. 8. Nucleation rate vs. supersaturation (in wt%) for lipid mixtures at 25.0 and 27.5°C. For abbreviations see Figure 2.

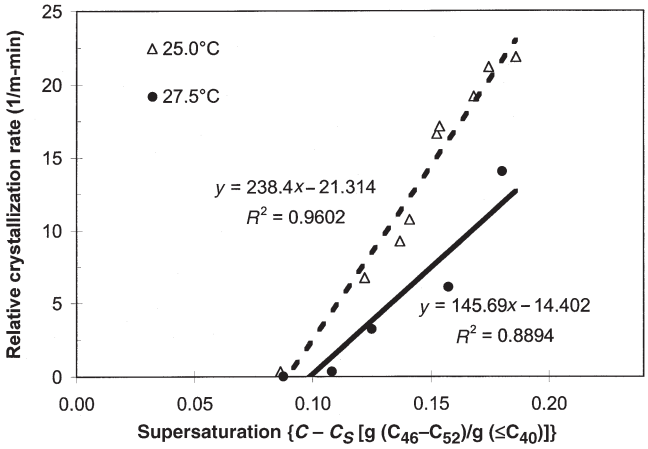

FIG. 10. Crystallization rate vs. supersaturation based on composition for mixtures of high-melting milk fat fraction (28S) with low-melting milk fat fraction (16L) at 25.0 and 27.5°C.

Instead, a simple linear relationship can be used to describe the kinetics for the supersaturation range higher than the critical value, as shown in Figure 10, where supersaturation is expressed as the ratio of long-/short-chain TAG. Note that a small change of TAG group ratio (long-chain to short-chain) affected the crystallization rate significantly, indicating that the TAG composition controlled crystallization in these complex lipid systems. A similar phenomenon occurred for nucleation, where, at a critical supersaturation (or supercooling) level, a large number of nuclei formed immediately (induction time = 0) followed by catastrophic crystallization.

ACKNOWLEDGMENT

Support from the Wisconsin Milk Marketing Board and the Center for Dairy Research at UW–Madison is gratefully appreciated.

REFERENCES

1. Bockisch, M., *Fats and Oils Handbook*, AOCS Press, Champaign, 1993.
2. Hettinga, D., Butter, in *Bailey's Industrial Oil & Fat Products, Vol. 3*, *Edible Oil & Fat Products and Application Technology,* edited by Y.H. Hui, John Wiley & Sons, New York, 1996, pp. 1–64.
3. Gresti, J., M. Bugaut, C. Maniongui, and J. Bezard, Composition of Molecular Species of Triacylglycerols in Bovine Milk Fat, *J. Dairy Sci. 76*:1850–1869 (1993).
4. Timms, R.E., Phase Behaviour of Fats and Their Mixtures, *Prog. Lipid Res. 23*:1–38 (1984).
5. Walstra, P., Fat Crystallization, in *Food Structure and Behavior,* edited by J.M. Blanshard and P. Liliford, Academic Press, Orlando, FL, 1987, pp. 67–85.
6. Mulder, H., and P. Walstra, *The Milk Fat Globule,* Centre for Agricultural Publishing and Documentation, Wageningen, The Netherlands, 1974.
7. Deffense, E., Milk Fat Fractionation Today: A Review, *J. Am. Oil Chem. Soc. 70*:1193–1201 (1993).
8. Mortensen, B.K., Physical Properties and Modification of Milk Fat, in *Developments in Dairy Chemistry 2: Lipids*, edited by P. Fox, Applied Science Publishers, New York, 1983, p. 159.
9. Hartel, R.W., *Crystallization in Foods*, Aspen, Gaithersburg, MD, 2001.
10. Lund, P., Analysis of Butterfat Triglycerides by Capillary Gas Chromatography, *Milchwissenschaft 43*:159–161 (1988).

[Received March 19, 2001; accepted December 13, 2002]